



Research Article

# Ailanthone inhibits bladder cancer tumor and cell proliferation, epithelial-mesenchymal transition, and activation of the Janus kinase/signal transducer and activator of transcription 3 signaling pathway

Jian Li, MD<sup>1\*</sup>, You Lv, MD<sup>1</sup>, Sheng Xue, PhD<sup>1\*</sup>, Wenyong Li, MD<sup>1</sup>, Xiaole Zhang, MD<sup>1</sup>

<sup>1</sup>Department of Urology, The First Affiliated Hospital of Bengbu Medical University, Bengbu, Anhui Province, China.

\*Corresponding authors:



Jian Li,  
Department of Urology, The First Affiliated  
Hospital of Bengbu Medical University,  
Bengbu, Anhui Province, China.  
lijian99109@hotmail.com



Sheng Xue  
Department of Urology, The First Affiliated  
Hospital of Bengbu Medical University,  
Bengbu, Anhui Province, China.  
bburo\_xs@163.com

Received: 23 August 2024  
Accepted: 24 December 2024  
Published: 12 February 2025

DOI  
10.25259/Cytojournal\_166\_2024

Quick Response Code:



## ABSTRACT

**Objective:** Ailanthone (AIL), a medicinal component with antitumor properties, was distilled from *Ailanthus altissima*. The aim of this work was to probe the cancer-fighting effect of AIL on bladder cancer (BC) cells and the molecular basis of this effect.

**Material and Methods:** We developed a subcutaneous BC mouse model and then administered AIL treatment. The effects of AIL on tumor tissue integrity and apoptosis were analyzed using hematoxylin and eosin (H&E) staining and terminal deoxynucleotidyl transferase dUTP nick-end labeling (TUNEL) staining methods. Furthermore, we investigated the effect of AIL on the Janus kinase/signal transducer and activator of transcription 3 (JAK/STAT3) pathway and associated proteins through quantitative reverse transcription polymerase chain reaction and Western blot analysis. Various concentrations of AIL were applied to BC cells, and its effects on cell survival, motility, and apoptosis were detected through cell counting kit-8 assay, Transwell assay, and flow cytometry. In addition, we examined the influence of AIL on apoptosis-related proteins and epithelial-mesenchymal transition (EMT)-related proteins in BC cells through Western blot analysis.

**Results:** AIL significantly suppressed the growth and migration of 5637 and T24 cells while promoting apoptosis ( $P < 0.05$ ,  $P < 0.01$ , and  $P < 0.001$ ). In addition, AIL increased the levels of cell death-associated proteins ( $P < 0.05$ ,  $P < 0.01$ , and  $P < 0.001$ ) and reversed EMT in BC cells. *In vivo*, AIL treatment reduced tumor growth and lowered the transcriptional levels of interleukin (IL)-6, IL-10, and IL-23, which are activation factors in the JAK/STAT3 signaling pathway. It also decreased the phosphorylation levels of JAK1, JAK2, and STAT3 in tumor tissues ( $P < 0.05$  and  $P < 0.01$ ).

**Conclusion:** AIL exhibits multiple anticancer effects, such as BC cell growth suppression, apoptosis enhancement, reversion of EMT reversion, tumor growth, and JAK/STAT3 pathway activation suppression.

**Keywords:** Ailanthone, Bladder cancer, Epithelial-mesenchymal transition, Janus kinase/signal transducer and activator of transcription 3, Proliferation

## INTRODUCTION

Bladder cancer (BC) is a well-known oncogenic tumor occurring within the genitourinary system. The 2020 Global Cancer Statistics report that BC ranks 9<sup>th</sup> and 13<sup>th</sup> in incidence and mortality, respectively, among all malignant tumors.<sup>[1]</sup> BC is mostly a urothelial malignancy.<sup>[2]</sup>

This is an open-access article distributed under the terms of the Creative Commons Attribution-Non Commercial-Share Alike 4.0 License, which allows others to remix, transform, and build upon the work non-commercially, as long as the author is credited and the new creations are licensed under the identical terms. © 2025 The Author(s). Published by Scientific Scholar.

After the surgical resection of bladder tumors, approximately 70% of BC cases recur. If BC is not treated properly, its degree of malignancy will increase.<sup>[3]</sup> Non-muscle-invasive BC tends to develop into muscle-invasive BC after multiple recurrences and metastasis. In addition to traditional surgical treatment, chemotherapy is an important treatment for BC.<sup>[4]</sup>

*Ailanthus altissima* is a species of *Ailanthus* in the family *Simaroubaceae*, which mainly thrives in temperate regions.<sup>[5]</sup> *A. altissima*, as a traditional medicinal plant, can be used to treat inflammation, viral infection, ulcers, cancer, and other diseases.<sup>[5]</sup> Ailanthone (AIL) is a medicinal component distilled from the bark of *A. altissima*<sup>[6]</sup> and exerts its anticancer effects mainly by mediating bio-targets and signaling pathways.<sup>[7]</sup>

Epithelial-mesenchymal transition (EMT) is a process that is often regulated by several signaling pathways. These pathways play a crucial role in the regulation of cell behavior during development and disease progression. One such pathway is the Janus kinase/signal transducer and activator of transcription 3 (JAK/STAT3) pathway, which is involved in various cellular processes such as proliferation, survival, and differentiation.<sup>[8,9]</sup>

Based on our understanding, no detailed mechanism of action of AIL against BC has been reported. Therefore, we assessed the significance of AIL on the survival rate and programmed cell death of 5637 and T24 cells. Furthermore, to probe the precise mechanism of AIL's anti-BC effect, we assessed alterations in the expression of proteins that regulate apoptosis and the engagement of the JAK/STAT3 signaling pathway.

## MATERIAL AND METHODS

### Animal experiments

A total of 18 BALB/c-nu mice (20–22 g, 6–8 weeks old) were purchased from Shanghai Model Organisms Center, Inc. (Shanghai, China). Human BC cells (5637 cells [iCell-h232, iCell Bioscience Inc., Shanghai, China]) were cultured to the logarithmic growth phase. The prepared BC cell suspension ( $1 \times 10^5$  cells/mL) was injected into the subcutaneous tissues of the mice, and the mice's growth and behavior were regularly monitored, with a specific focus on tracking tumor progression. Using a random number table, we assigned the 18 inoculated mice to three experimental groups: Control group, 10 mg/kg AIL treatment group (CFN97561, ChemFaces, Wuhan, China), and 15 mg/kg AIL treatment group.<sup>[10]</sup> The mice in the 10 mg/kg AIL group were intraperitoneally injected with 10 mg/kg AIL daily, whereas those in the 15 mg/kg AIL group were intraperitoneally injected with 15 mg/kg AIL daily. The mice in the control group were intraperitoneally injected with an equal volume of saline daily. After 21 days of inoculation, the experiment

was completed. The mice were euthanized through an intraperitoneal injection of pentobarbital sodium (3 mg/mL) at a dose of 110 mg/kg (P3761, Sigma-Aldrich, St. Louis, Missouri, USA). Tumor tissues were extracted for subsequent histopathological and molecular biological analyses. Animal experiments complied with the principles of animal protection. This study has been approved by the Committee of Bengbu Medical University, approval no.: 2023116.

### Cell culture

Human BC cell lines, including 5637 cells (iCell-h232), T24 cells (iCell-h208), and the bladder epithelial cell line Simian Virus 40 (SV40) transformed Human Uroepithelial Cell Line 1 (SV-HUC-1), were purchased from iCell Bioscience Inc. (Shanghai, China). All cells were cultured in specialized medium. The above cells were cultured at 37°C with 5% carbon dioxide (CO<sub>2</sub>). All cells have been subjected to short tandem repeat authentication and tested negative for mycoplasma.

AIL samples (CFN97561; purity  $\geq 98\%$ ) were obtained from ChemFaces (Wuhan, China). A stock solution of AIL was prepared in phosphate-buffered saline (PBS) and stored at  $-20^\circ\text{C}$ . For experimental purposes, various concentrations of AIL (0, 0.2, 0.4, 0.8, 1.6, and 3.2  $\mu\text{M}$ ) were prepared in PBS and then added to the cell culture medium as required.

### Quantitative reverse transcription polymerase chain reaction (qRT-PCR)

Total ribonucleic acid (RNA) was isolated from BC tumors or cells with an RNA extraction kit (DP424, TIANGEN, Beijing, China). RNA was converted into complementary DNA (cDNA) with a special kit (KR107, TIANGEN, Beijing, China), and specific primers for target and reference genes (*Glyceraldehyde-3-phosphate dehydrogenase [GAPDH]*) were designed. Polymerase chain reaction mixtures were prepared, comprising cDNA templates, primers, and a fluorescent DNA-binding dye specific to the target gene (SYBR Green). Ct values were recorded for each sample, and target gene expression was standardized against the reference gene using the  $2^{-\Delta\Delta\text{Ct}}$  method. Primer sequences utilized in this study are shown in Table 1.

### Western blot

Proteins were first separated through electrophoresis and subsequently transferred to a polyvinylidene fluoride (PVDF) membrane (FFP19, Beyotime, Shanghai, China). The membrane was soaked in 5% bovine serum albumin (BSA) (P0007, Beyotime, Shanghai, China) at room temperature (25°C) for 1 h to block nonspecific binding. Then, the membrane was incubated with the following primary antibodies at 4°C overnight: E-cadherin

**Table 1:** Names and sequences of primers employed in this study.

Primer names	Primer sequence (5quenc
Mouse-IL-6-F	AACCACGGGCTTCCCTACTT
Mouse-IL-6-R	TCTGTTGGGAGTGGTATCCTCTGT
Mouse-IL-10-F	GGTTGCCAAGCCTTATCGGA
Mouse-IL-10-R	TTCAGCTTCTCACCCAGGGA
Mouse-IL-23-F	CAGGTATGAAGTAGGGGCGTG
Mouse-IL-23-R	GGGACTGAGGCTTGAATCT
GAPDH-F	TGGAGAAACCTGCCAAGTATG
GAPDH-R	GGAGACAACCTGGTCCTCAG

IL-6: Interleukin-6, IL-10: Interleukin-10, IL-23: Interleukin-23, GAPDH: Glyceraldehyde-3-phosphate dehydrogenase. F: Forward, R: Reverse, A: Adenine, C: Cytosine, G: Guanine, T: Thymine

(E-cad; 1:1000; cat no. EM0502, HuaBio), N-cadherin (N-cad; 1:1000; cat no. M1304-1, HuaBio, Hangzhou, China), vimentin (1:1000; cat no. ET1610-39, HuaBio, Hangzhou, China), caspase-9 (1:1000; cat no. ER60008, HuaBio, Hangzhou, China), caspase-3 (1:500; cat no. ab2302, Abcam, Cambridge, UK), B-cell lymphoma 2 (Bcl-2) (1:2000; cat no. 12789-1-AP, Proteintech, Wuhan, China), Bcl-2-associated X protein (Bax) (1:1000; cat no. 50599-1-AP, Proteintech, Wuhan, China), JAK1 (1:1000; cat no. 66466-1-Ig, Proteintech, Wuhan, China), JAK2 (1:1000; cat no. ab108596, Abcam, Cambridge, UK), phosphorylation-JAK1 (p-JAK1) (1:1000; cat no. ab278781, Abcam, Cambridge, UK), p-JAK2 (1:1000; cat no. Ab32101, Abcam, Cambridge, UK), STAT3 (1:1000; cat no. Ab68153, Abcam, Cambridge, UK), p-STAT3 (1:1000; cat no. ab76315, Abcam, Cambridge, UK), and GAPDH (1:1000; cat no. ab181602, Abcam, Cambridge, UK) at 4°C overnight. Subsequently, Horseradish peroxidase (HRP)-conjugated secondary antibodies (1:2000; cat no. ZB-2305, ZB-2301, ZSGB-BIO, Beijing, China) were applied. Finally, a chemiluminescent reagent (E-IR-R300, Elabscience, Wuhan, China) was added and visualized using a gel imaging system (Azure C300, Azure Biosystems, Dublin, California, USA). The intensities of the protein bands were quantitatively analyzed using ImageJ software (version 4.5f, National Institutes of Health (NIH), Bethesda, Maryland, USA). GAPDH was selected as the standard for the normalization of protein bands.

#### Cell counting kit-8 (CCK-8) assay

T24 and 5637 cells were cultured in 96 well plates ( $1 \times 10^3$  cells/well). Then, the plates were placed in a culture environment with 5% CO<sub>2</sub> at 37°C temperature. A CCK-8 solution (C0037, Beyotime, Shanghai, China) was introduced into the plates at regular intervals, and 5637 and T24 cells were incubated in the dark for 2 h. A microplate reader (Cmax plus3000, Molecular Devices Corporation, San Jose,

California, USA) was used to measure the absorbance of BC cells' viability at 450 nm.

#### Transwell assay

A Transwell plate was soaked in a mild cell culture medium (serum-free medium). The target cells in the medium were suspended evenly at an appropriate concentration ( $1 \times 10^5$  cells/mL). After the pretreated Transwell plate was inverted, we added the cell suspension to the upper chamber, preventing leakage and bubble formation. The Transwell plate was placed in a humidified CO<sub>2</sub> incubator (Heracell 240i, Thermo Fisher Scientific, Waltham, Massachusetts, USA) at 37°C with 5% CO<sub>2</sub> under appropriate culture conditions. The cells were incubated for a certain period as required and allowed to migrate from the upper chamber through the membrane to the lower chamber. Cell migration was stopped by removing the plate from the incubator and adding PBS to the lower chamber. The cells were stained with 1% crystal violet solution, and the migrated cells were observed under a microscope (IX83, Olympus, Tokyo, Japan).

#### Flow cytometry

First, collect and wash the cells to be analyzed, fix them with 70% cold ethanol, and then stain with Annexin V conjugated with fluorescein isothiocyanate (Annexin V-FITC) and propidium iodide (PI) dyes (C1062L, Beyotime, Shanghai, China). Annexin V labels early apoptotic cells, while PI stains late apoptotic or necrotic cells. After staining, analyze the apoptotic status of the cells by detecting different fluorescence intensities using a flow cytometer.

The cells from the culture were collected and resuspended in PBS, and their concentration was adjusted to  $1 \times 10^6$  cells/mL. The cells were mixed with 10 μM 5,5',6,6'-tetrachloro-1,1',3,3'-tetraethylbenzimidazolylcarbocyanine iodide (JC-1) dye (C2003S, Beyotime, Shanghai, China) and incubated at 37°C for 30 min away from light. After incubation, unbound dye was removed through centrifugation, and the cells were washed twice with PBS and resuspended. The cell samples were transferred to a flow cytometer (BECKMAN, Beckman Coulter Co., LTD., California, USA), and JC-1 green fluorescence (monomeric state; excitation wavelength is approximately 490 nm) and red fluorescence (aggregated state; excitation wavelength is approximately 525 nm) were recorded. Finally, membrane potential was calculated according to changes in fluorescence intensity, and fluorescence ratios were compared between the treatment and control groups.

#### Hematoxylin and eosin (H&E) staining

Tissues were fixed for 4 h with 4% paraformaldehyde (P1110, Solarbio, Beijing, China) and placed in a series of increasing

concentrations of alcohol to gradually remove water. We cleaned the tissues with an appropriate clearing agent and immersed them in liquid paraffin to increase their firmness for sectioning. The paraffin blocks were cut into 5  $\mu\text{m}$  sections with a microtome (RM2255, Leica Microsystems, Wetzlar, Germany). The sections were stained with H&E (G1120, Solarbio, Beijing, China), dehydrated, and cleared. A coverslip was used to encapsulate and protect the sections. The H&E-stained sections were observed under a microscope (DM2500, Leica Microsystems, Wetzlar, Germany) and analyzed the morphological structure of the tissues.

### Terminal deoxynucleotidyl transferase dUTP nick-end labeling (TUNEL) staining

The tumor tissue paraffin sections were deparaffinized in xylene for 5 min and washed with ethanol gradients of 100%, 95%, 90%, 80%, and 70% for 3 min for each gradient. Afterward, the sections were rinsed twice with PBS. Proteinase K treatment was applied to the tumor tissues for 30 min, washed with PBS twice, and immersed in a blocking solution. After 10 min of incubation at room temperature, the sections were rinsed twice with PBS. A mixture of 2  $\mu\text{L}$  of terminal deoxynucleotidyl transferase (TdT) and 48  $\mu\text{L}$  of dUTP solution (11684817910, Roche, Beijing, China) was then applied to the sections, which were then incubated in a humid chamber for 1 h at room temperature. Subsequently, the sections were washed 3 times with PBS before immunostaining with secondary antibodies and 3,3'-diaminobenzidine (DAB) chromogen under a microscope (CX53, Olympus, Tokyo, Japan) for photography. Quantitative analysis of TUNEL-positive cells was performed using ImageJ software (version 4.5f, NIH, Bethesda, Maryland, USA).

### Statistical analysis of data

Statistical analysis was conducted using GraphPad Prism software (version 8.0, GraphPad Prime Inc., San Diego, California, USA). The *t*-test was used for comparisons between two groups, whereas one-way analysis of variance with Tukey's *post hoc* test was used for comparisons involving more than two groups. Data were presented as mean  $\pm$  standard deviation, and  $P < 0.05$  was considered statistically significant.

## RESULTS

### Effect of AIL on the proliferation of BC cells

AIL inhibited 5637 and T24 cell viability in proportion to the dose ( $P < 0.05$ ,  $P < 0.01$ , and  $P < 0.001$ ; [Figure 1a and b]). Meanwhile, we focused the investigation on the SV-HUC-1 cells to evaluate the cytotoxic effects of

AIL on normal bladder epithelial cells. The data indicated that an AIL dose of 0.2 and 0.4  $\mu\text{M}$  showed low cytotoxicity to normal bladder epithelial cells, and the toxic effect on normal bladder epithelial cells increased significantly with AIL dose ( $P < 0.001$ ; [Figure 1c]). Therefore, AIL with safe action concentrations of 0.2 and 0.4  $\mu\text{M}$  were selected for the experimental groups in subsequent experiments.

### AIL suppressed the growth of tumors *in vivo*

Figures 2a-c demonstrate that AIL suppressed the growth of subcutaneous tumors in mice and substantially reduced tumor volume and weight. The 15 mg/kg AIL group exhibited the most significant inhibitory effect ( $P < 0.001$ ). H&E staining revealed structural damage, irregular cell arrangement, and necrotic areas in tumors treated with AIL [Figure 2d]. TUNEL staining further showed a notable rise in cell death in tumors treated with various doses of AIL ( $P < 0.01$  and  $P < 0.001$ ; [Figure 2e and f]).

### AIL suppressed the migration of BC cells and promoted the EMT process

The migration capacity of AIL on BC cells was analyzed through Transwell assay. AIL clearly suppressed the migratory capabilities of the 5637 and T24 cells ( $P < 0.001$ ; [Figure 3a and b]). Malignant tumor cells often enhance their migratory and invasive capabilities through EMT. We investigated the expression levels of E-cad, N-cad, and vimentin. The findings showed that as the concentration of AIL increased in the 5637 and T24 cells, N-cad and vimentin expression levels decreased, which were positively associated with EMT. Conversely, the expression level of E-cad, which is negatively connected with EMT, increased with AIL concentration ( $P < 0.05$ ,  $P < 0.01$ , and  $P < 0.001$ ; [Figure 3c-f]).

### AIL induced apoptosis in BC cells

Figures 4a and b reveal that apoptosis rates in 5637 and T24 cells increased progressively with AIL concentration, and significant increases were observed at 0.2 and 0.4  $\mu\text{M}$  ( $P < 0.05$  and  $P < 0.01$ ).

To assess the role of AIL on apoptosis-related proteins, we examined its effect on the caspase family. AIL treatment resulted in a significant and concentration-dependent increase in the levels of cleaved caspase-3 and caspase-9 in the 5637 and T24 cells ( $P < 0.05$ ,  $P < 0.01$ , and  $P < 0.001$ ; [Figure 4c-f]), indicating that AIL induces apoptosis through the caspase cascade pathway.

Moreover, AIL treatment led to a rise in Bax protein levels and a reduction in Bcl-2 protein levels in the 5637 and T24 cells ( $P < 0.05$ ,  $P < 0.01$ , and  $P < 0.001$ ;

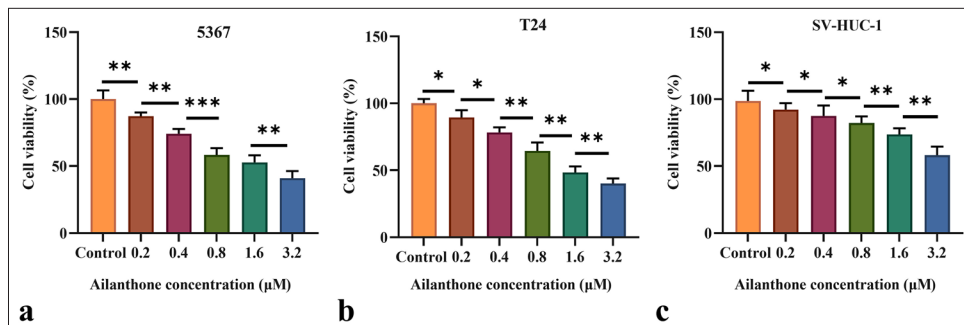


**Figure 1:** AIL effectively inhibit the proliferation in 5637, T24, and SV-HUC-1 cells. (a-c) The effects of AIL on the proliferation of 5637 (a), T24 (b), and SV-HUC-1 (c) cells were assessed ( $n = 6$ ). (\* $P < 0.05$ , \*\* $P < 0.01$ , \*\*\* $P < 0.001$ ). AIL: Ailanthone; SV-HUC-1: Simian Virus 40 (SV40) transformed Human Uroepithelial Cell Line 1.

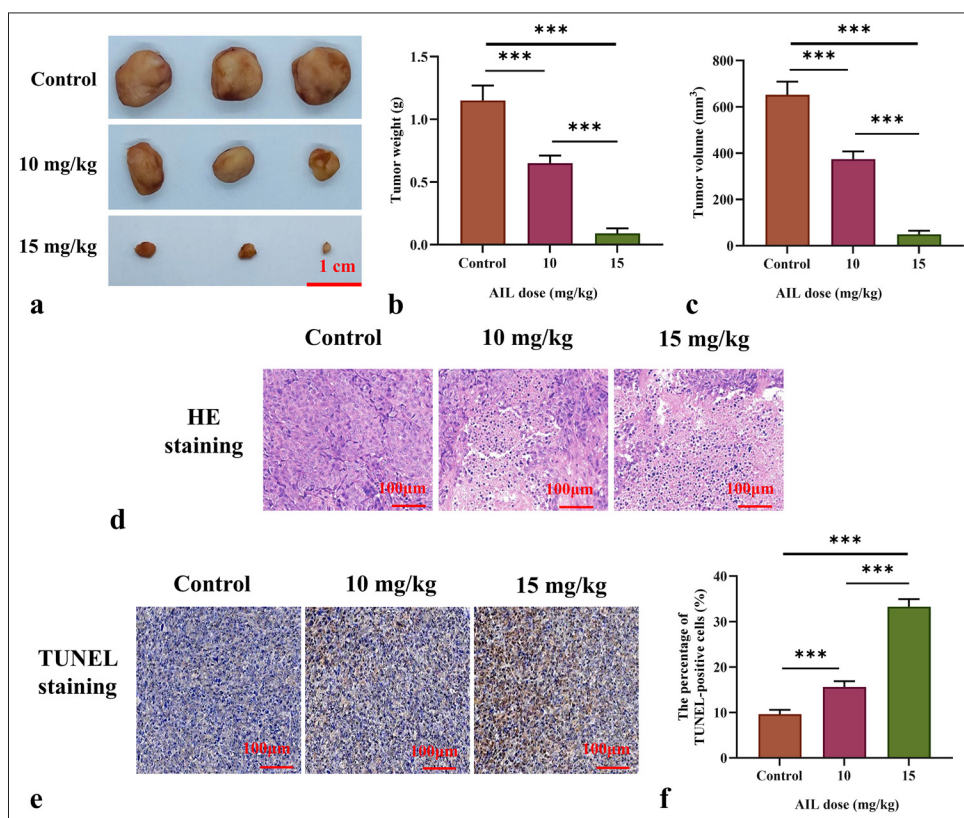


**Figure 2:** AIL suppresses the growth of tumors *in vivo*. (a-c) Determination of tumor size and weight in mice treated with different doses of AIL. (d) Hematoxylin and eosin-stained images of tumor tissues, 50x. (e and f) Pictures of TUNEL staining of tumor tissue, 50x. ( $n = 6$ ). \*\*\* $P < 0.001$ . AIL: Ailanthone, TUNEL: Terminal deoxynucleotidyl transferase deoxyuridine triphosphate (dUTP) nick-end labeling.

[Figure 4c-f)]. [Figures 5a-c] demonstrate that AIL treatment (0.2 and 0.4 μM) caused a notable reduction in membrane potential across the mitochondria in the 5637 and T24 cells ( $P < 0.05$ ,  $P < 0.01$ , and  $P < 0.001$ ), suggesting that AIL induces apoptosis through the mitochondrial pathway.

### AIL participates in the signaling transduction of the JAK/STAT3 pathway in tumor tissues

We assessed the messenger RNA (mRNA) levels of Interleukin (IL)-6, IL-10, and IL-23, key activation factors in the JAK/STAT3 pathway, in tumor tissue using qRT-PCR.

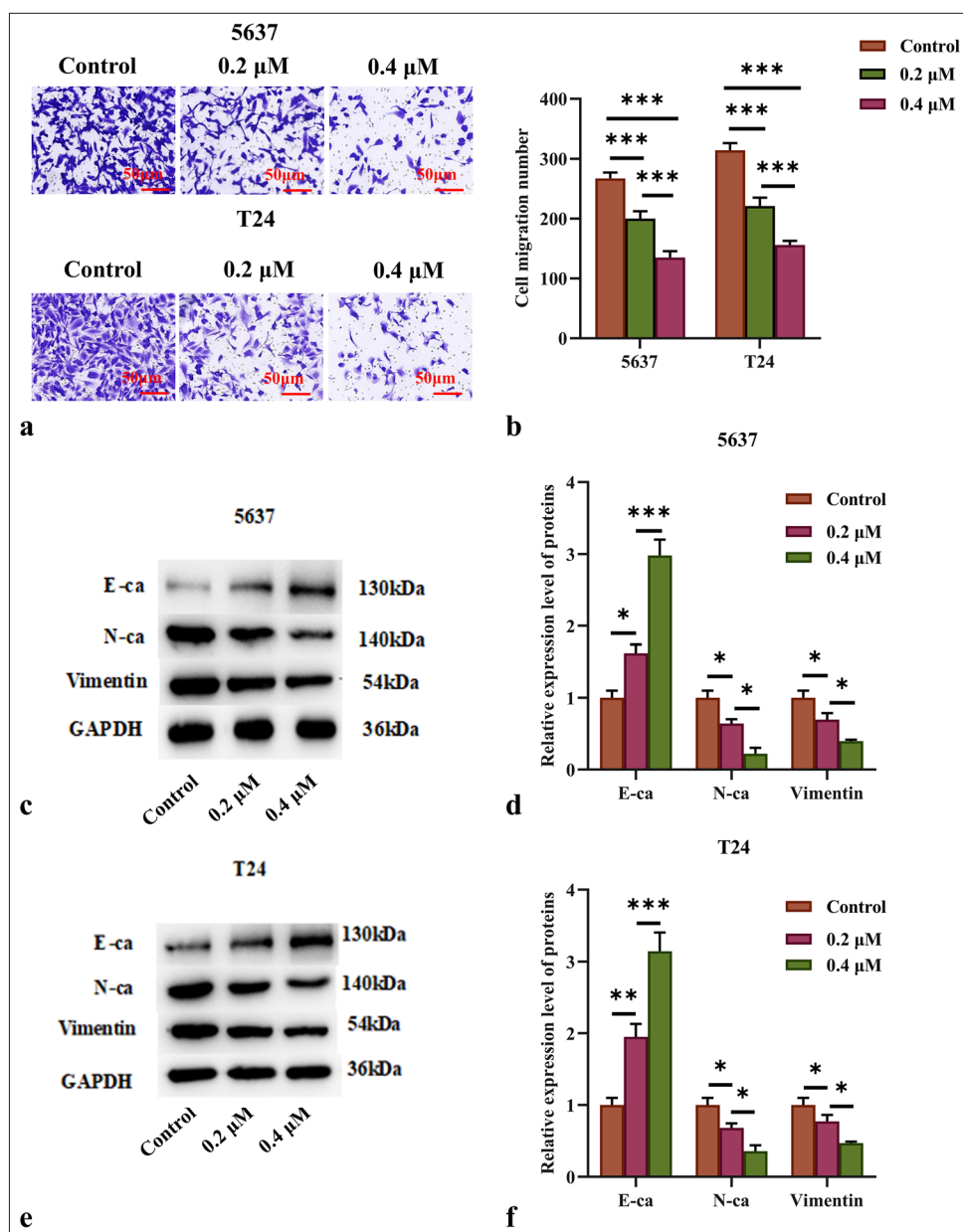


**Figure 3:** AIL suppressed the migration of BC cells. (a and b) The effect of AIL on the migration capabilities of 5637 and T24 cells was evaluated ( $n = 3$ ). (c-f) The expression levels of proteins associated with EMT (E-cad, N-cad, and vimentin) were measured ( $n = 6$ ). (\* $P < 0.05$ , \*\* $P < 0.01$ , \*\*\* $P < 0.001$ ). E-cad: E-cadherin, N-cad: N-cadherin, GAPDH: *Glyceraldehyde-3-phosphate dehydrogenase*.

As shown in Figure 6a-c, AIL treatment at 10 and 15 mg/kg markedly reduced the mRNA expression of IL-6, IL-10, and IL-23 ( $P < 0.05$  and  $P < 0.01$ ).

In addition, Western blot analysis was used to assess the role of AIL on the protein expression and phosphorylation of JAK1, JAK2, and STAT3. The results revealed that AIL treatment led to a notably reduce in the phosphorylation levels of JAK1, JAK2, and STAT3 across various concentrations, while the total protein levels of these

molecules remained unchanged ( $P < 0.05$  and  $P < 0.01$ ; [Figure 6d-g]).

## DISCUSSION

*A. altissima*, a medicinal plant native to China, yields AIL, which possesses anticancer properties.<sup>[6,11,12]</sup> However, AIL's effects against BC and related molecular mechanisms have not been explored. This investigation focused on elucidating AIL's anticancer properties against BC cells.

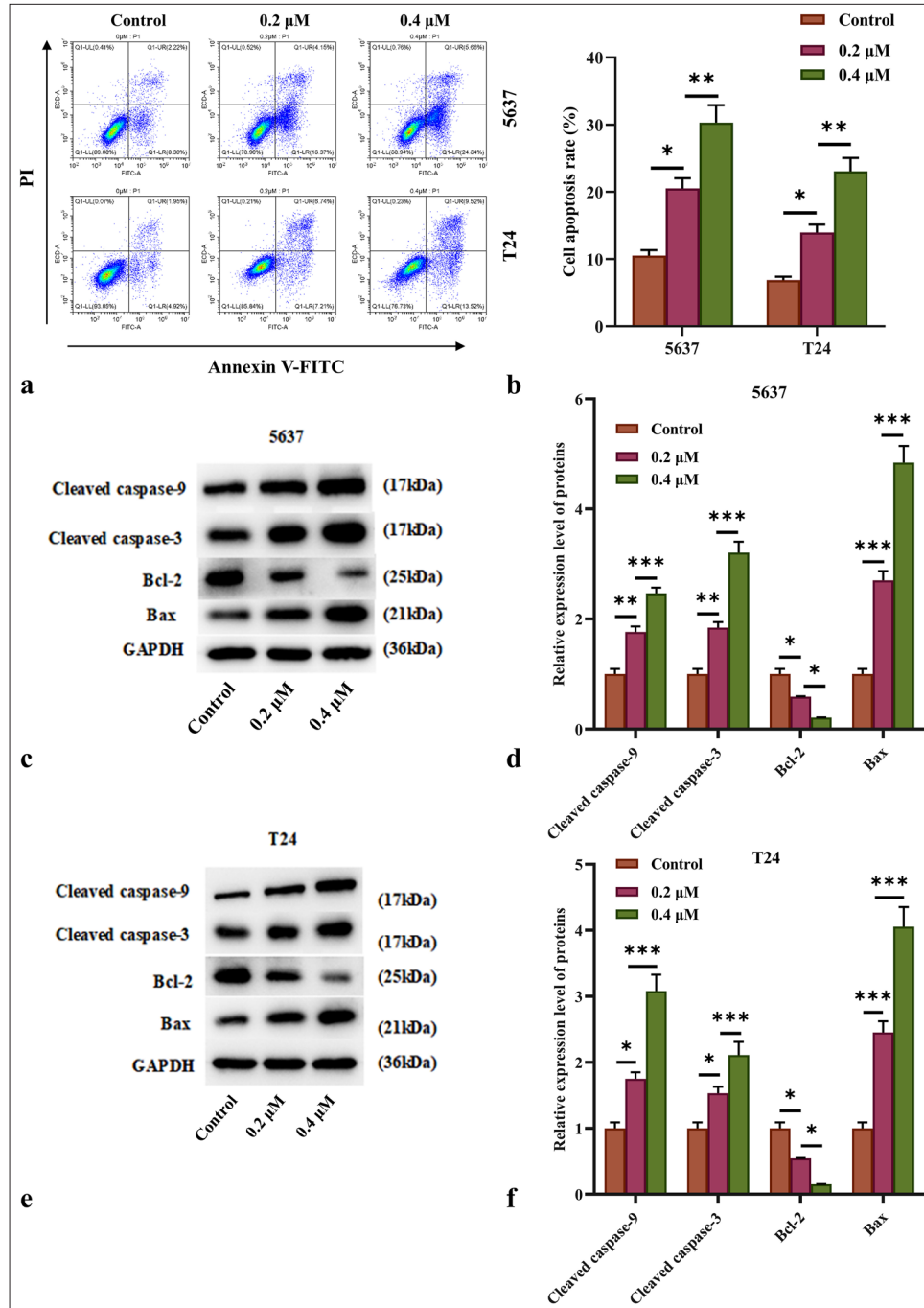


**Figure 4:** AIL induced apoptosis of BC cells. (a and b) Apoptosis rates of 5637 and T24 cells under treatment with AIL were assessed by flow cytometry ( $n = 3$ ). (c-f) The expression levels of programmed cell death proteins, including caspase-3, caspase-9, Bcl-2, and Bax, were measured ( $n = 6$ ) \* $P < 0.05$ , \*\* $P < 0.01$ , \*\*\* $P < 0.001$ . AIL: Ailanthone, BC: Bladder cancer, Bcl-2: B-cell lymphoma 2, Bax: Bcl-2-associated X protein

Through a CCK-8 assay, we examined how AIL affected the growth of BC cell lines 5637 and T24. AIL inhibited the proliferation of the cell lines in accordance with the dose. Similarly, Ding *et al.* corroborated the inhibition proportional to the concentration of AIL on colorectal cancer

cell proliferation.<sup>[13]</sup> Furthermore, we examined the cytotoxic effects of AIL on SV-HUC-1 cells to determine the optimal concentration range for its action. Our findings revealed that at low concentrations (0.2 and 0.4 μM), AIL exhibited lower levels of inhibitory effects on the viability of SV-HUC-1 cells

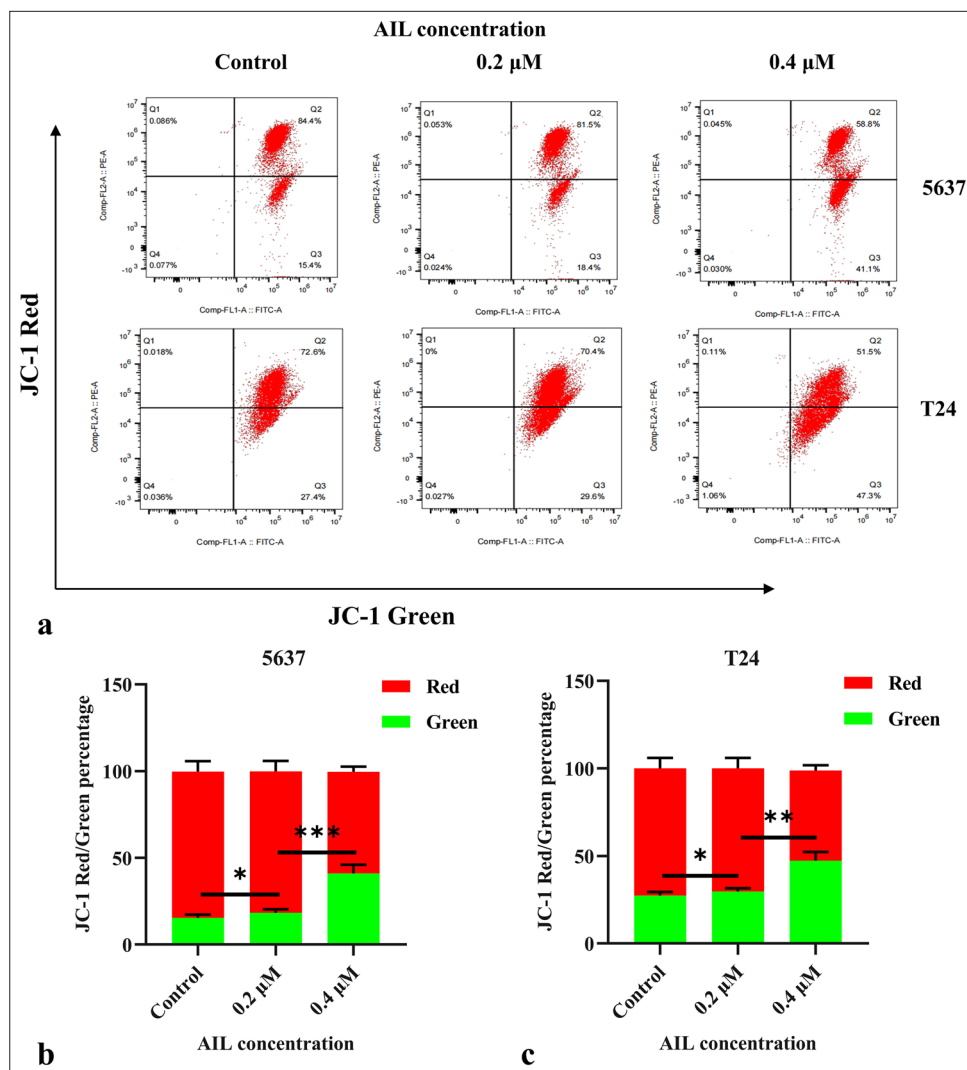


**Figure 5:** AIL reduces membrane potential across the mitochondria in BC cells. (a-c) The effect of AIL on the membrane potential across the mitochondria in BC cells was examined ( $n = 3$ ;  $*P < 0.05$ ,  $**P < 0.01$ , and  $***P < 0.001$ ). AIL: Ailanthone, BC: Bladder cancer, JC-1: 5,5',6,6'-Tetrachloro-1,1',3,3'-tetraethylbenzimidazolylcarbocyanine iodide.

than on the viability of 5637 and T24 cells, demonstrating lower cytotoxicity toward SV-HUC-1 cells. These results suggest that AIL demonstrates greater sensitivity toward tumor cells and lower toxicity toward normal cells at low concentrations.

Apoptosis is highly regulated at the gene level and can orderly and effectively eliminate damaged (cells with DNA damage) and senescent cells, maintaining the stability of the milieu interne.<sup>[14]</sup> The main pathways of apoptosis include endogenous and exogenous pathways. Caspases are central to the process of programmed cell death because they are initiators and executors.<sup>[15]</sup> These pathways induce apoptosis by activating caspases into a common terminal pathway.<sup>[16]</sup>

The mitochondrial apoptotic pathway (endogenous) is mediated and initiated within cells by intracellular signals that can be stimulated by various stress stimuli.<sup>[17]</sup>

Understanding and applying apoptosis mechanisms can facilitate the removal of tumor cells' malignant potential. In this investigation, we initially demonstrated through flow cytometry analysis that the apoptosis rate of both BC cell lines increased after AIL treatment. Subsequent flow cytometry analysis revealed a reduction in mitochondrial membrane potential in the 5637 and T24 cell lines on AIL exposure.

The STAT family participates in the development of tumors related to inflammation and has a vital function in the specific initiation and preservation of a cancer-causing inflammatory environment.<sup>[18,19]</sup>

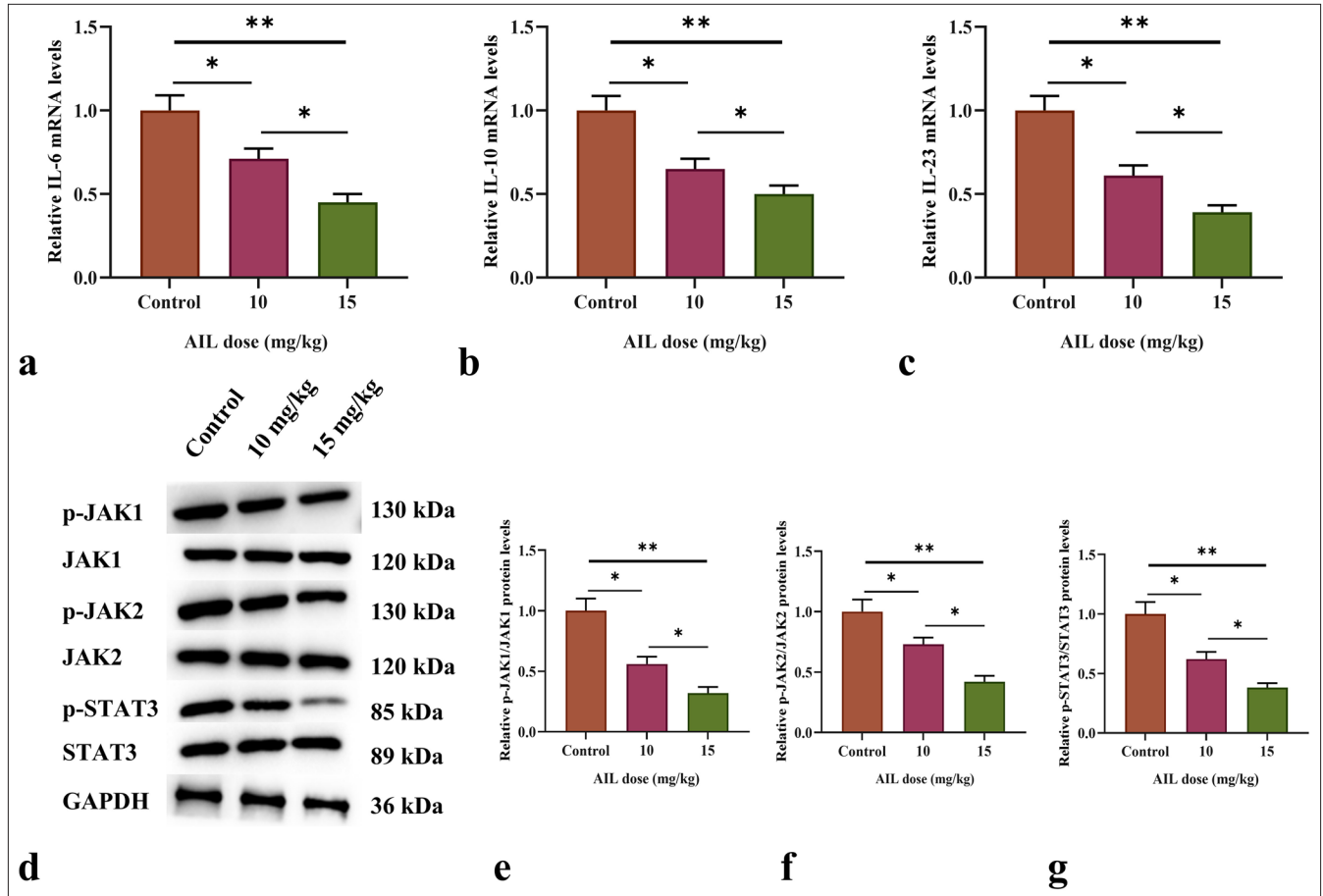


**Figure 6:** AIL suppresses the signaling transduction of the JAK/STAT3 pathway. (a-c) The messenger RNA (mRNA) levels of IL-6, IL-10, and IL-23 in tumor tissues after treatment with different doses of AIL. (d-g) The protein expression and phosphorylation levels of JAK1, JAK2, and STAT3 in tumor tissues following treatment with varying doses of AIL. ( $n = 6$ ). ( $*P < 0.05$  and  $**P < 0.01$ ). AIL: Ailanthone, IL: Interleukin, JAK1: Janus kinase 1, JAK2: Janus kinase 2, STAT3: Signal transducer and activator of transcription 3, p-JAK1: Phosphorylated JAK1, p-JAK2: Phosphorylated JAK2, p-STAT3: Phosphorylated STAT3.

STAT3 has a high correlation with inflammation-related tumors and participates in various pro-inflammatory cytokines and growth factor-stimulated oncogenic signaling and intracellular signal transduction pathways *in vivo*.<sup>[20]</sup> STAT3 regulates tumor cell proliferation, survival, invasion, metastasis, and angiogenesis by targeting different genes.<sup>[21]</sup> The activation of the STAT3 pathway can promote invasion by tumor cells and their metastasis by down-regulating E-cad and up-regulating vimentin.<sup>[22]</sup> To date, JAK and STAT3 inhibitors inhibit the progression of cancer by targeting STAT3 pathways.<sup>[23]</sup> The results of our study reveal a considerable effect of AIL treatment on the JAK/STAT3 signaling pathway in tumor tissues. Through qRT-PCR analysis, we observed a pronounced reduction in the mRNA expression levels of key activation factors, namely, IL-6, IL-10, and IL-23, in the tumor tissue JAK/STAT3 pathway after treatment with 10 and 15 mg/kg AIL. This result suggests that AIL effectively modulates the transcriptional regulation of these cytokines, exhibiting its potential to attenuate

inflammatory and immune responses associated with tumor growth. Furthermore, Western blot experiments provided insights into the post-translational modifications of JAK1, JAK2, and STAT3 proteins in response to AIL treatment. Remarkably, AIL exhibited a dose-dependent inhibition of phosphorylation levels for these signaling molecules without affecting their overall protein expression. These findings indicate that AIL intervenes in the activation of JAK/STAT3 signaling by impeding phosphorylation cascades, consequently disrupting downstream cellular responses involved in tumor progression. The observed reduction in the transcriptional levels of pro-inflammatory cytokines and the inhibition of JAK/STAT3 pathway activation align with previous studies highlighting the role of this signaling cascade in promoting tumor growth. The disrupted structural integrity and increased cell death observed in tumor tissues after AIL treatment, as evidenced by H&E and TUNEL staining, further support the antitumor potential of AIL.

In conclusion, our research sheds light on the molecular mechanisms driving AIL's antitumor effects. AIL targets the JAK/STAT3 signaling pathway and affects critical cytokine levels, demonstrating its potential as a therapeutic agent for tumors. To fully explore AIL's clinical relevance in cancer treatment, additional studies, including comprehensive mechanistic investigations and clinical trials, are necessary.

## SUMMARY

AIL exhibits a range of anticancer effects, including inhibiting BC cell growth, inducing apoptosis, suppressing EMT, and modulating tumor growth and JAK/STAT3 signaling.

## AVAILABILITY OF DATA AND MATERIALS

Data and materials to support the findings of this study are available on reasonable request from the corresponding author.

## ABBREVIATIONS

A: Adenine  
 AIL: Ailanthone  
 Bax: Bcl-2-associated X protein  
 BC: Bladder cancer  
 Bcl-2: B-cell lymphoma 2  
 C: Cytosine  
 E-cad: E-cadherin  
 F: Forward  
 G: Guanine  
 GAPDH: Glyceraldehyde-3-phosphate dehydrogenase  
 H&E: Hematoxylin and eosin  
 IL-10: Interleukin-10  
 IL-23: Interleukin-23  
 IL-6: Interleukin-6  
 JAK1: Janus kinase 1  
 JAK2: Janus kinase 2  
 JC-1: 5,5',6,6'-Tetrachloro-1,1',3,3'-tetraethylbenzimidazolyl carbocyanine iodide.  
 N-cad: N-cadherin  
 p-JAK1: Phosphorylated JAK1  
 p-JAK2: Phosphorylated JAK2  
 p-STAT3: Phosphorylated STAT3  
 R: Reverse  
 STAT3: Signal transducer and activator of transcription 3  
 SV-HUC-1: Simian Virus 40 (SV40) transformed Human Uroepithelial Cell Line 1  
 T: Thymine  
 TUNEL: Terminal deoxynucleotidyl transferase dUTP nick-end labeling

## AUTHOR CONTRIBUTIONS

JL (First Author): Conceptualization, methodology, software, investigation, formal analysis, funding acquisition, writing - original draft; YL: Data curation, writing - original draft; SX: Visualization, investigation; WL: Software, validation; XLZ: Visualization, writing - review and editing.

## ETHICS APPROVAL AND CONSENT TO PARTICIPATE

This study has been approved by the Committee of Bengbu Medical University, approval no.: 2023116, dated March 13, 2023. Consent to participate is not required as there are no patients in this study.

## ACKNOWLEDGMENT

Not applicable.

## FUNDING

Natural Science Research Project of Anhui Educational Committee (KJ2021A0793).

## CONFLICT OF INTEREST

The authors declare no conflict of interest.

## EDITORIAL/PEER REVIEW

To ensure the integrity and highest quality of CytoJournal publications, the review process of this manuscript was conducted under a **double-blind model** (authors are blinded for reviewers and vice versa) through an automatic online system.

## REFERENCES

1. Sung H, Ferlay J, Siegel RL, Laversanne M, Soerjomataram I, Jemal A, *et al.* Global Cancer Statistics 2020: GLOBOCAN estimates of incidence and mortality worldwide for 36 cancers in 185 countries. *CA Cancer J Clin* 2021;71:209-49.
2. Cumberbatch MG, Jubber I, Black PC, Esperto F, Figueroa JD, Kamat AM, *et al.* Epidemiology of bladder cancer: A systematic review and contemporary update of risk factors in 2018. *Eur Urol* 2018;74:784-95.
3. Ito A, Shintaku I, Satoh M, Ioritani N, Aizawa M, Tochigi T, *et al.* Prospective randomized phase II trial of a single early intravesical instillation of pirarubicin (THP) in the prevention of bladder recurrence after nephroureterectomy for upper urinary tract urothelial carcinoma: The THP Monotherapy Study Group Trial. *J Clin Oncol* 2013;31:1422-7.
4. Liu L, Xu L, Wu D, Zhu Y, Li X, Xu C, *et al.* Impact of tumour stroma-immune interactions on survival prognosis and response to neoadjuvant chemotherapy in bladder cancer. *EBioMedicine* 2024;104:105152.

5. Li X, Li Y, Ma S, Zhao Q, Wu J, Duan L, *et al.* Traditional uses, phytochemistry, and pharmacology of *Ailanthus altissima* (Mill.) Swingle bark: A comprehensive review. *J Ethnopharmacol* 2021;275:114121.
6. Ding H, Yu X, Hang C, Gao K, Lao X, Jia Y, *et al.* Ailanthone: A novel potential drug for treating human cancer. *Oncol Lett* 2020;20:1489-503.
7. Wang C, Yi T, Li X, Cui J, Li B, Qin Y, *et al.* Ailanthone synergizes with PARP1 inhibitor in tumour growth inhibition through crosstalk of DNA repair pathways in gastric cancer. *J Cell Mol Med* 2024;28:e18033.
8. Ma J, Liu M, Chen Z, Liu S, Yang H, Duan M. NANOG regulate the JAK/STAT3 pathway to promote trophoblast cell migration and epithelial-mesenchymal transition (EMT) in hypertensive disorders of pregnancy (HDP) through protein interaction with CDK1. *Am J Reprod Immunol* 2024;91:e13863.
9. Kim MS, Lee HS, Kim YJ, Lee DY, Kang SG, Jin W. MEST induces Twist-1-mediated EMT through STAT3 activation in breast cancers. *Cell Death Differ* 2019;26:2594-606.
10. Di J, Bo W, Wang C, Liu C. Ailanthone increases cisplatin-induced apoptosis and autophagy in cisplatin resistance non-small cell lung cancer cells through the PI3K/AKT/mTOR pathway. *Curr Med Chem* 2024.
11. Wang S, Cui Q, Chen X, Zhu X, Lin K, Zheng Q, *et al.* Ailanthone inhibits cell proliferation in tongue squamous cell carcinoma via PI3K/AKT pathway. *Evid Based Complement Alternat Med* 2022;2022:3859489.
12. Zhao L, Zhu Y, Tao H, Chen X, Yin F, Zhang Y, *et al.* Ailanthone ameliorates pulmonary fibrosis by suppressing JUN-dependent MEOX1 activation. *Acta Pharm Sin B* 2024;14:3543-60.
13. Ding H, Yu X, Yan Z. Ailanthone suppresses the activity of human colorectal cancer cells through the STAT3 signaling pathway. *Int J Mol Med* 2022;49:21.
14. Fuchs Y, Steller H. Programmed cell death in animal development and disease. *Cell* 2011;147:742-58.
15. Ai Y, Meng Y, Yan B, Zhou Q, Wang X. The biochemical pathways of apoptotic, necroptotic, pyroptotic, and ferroptotic cell death. *Mol Cell* 2024;84:170-9.
16. Kesavardhana S, Malireddi RK, Kanneganti TD. Caspases in cell death, inflammation, and pyroptosis. *Annu Rev Immunol* 2020;38:567-95.
17. Victorelli S, Salmonowicz H, Chapman J, Martini H, Vizioli MG, Riley JS, *et al.* Apoptotic stress causes mtDNA release during senescence and drives the SASP. *Nature* 2023;622:627-36.
18. Lu R, Zhang YG, Sun J. STAT3 activation in infection and infection-associated cancer. *Mol Cell Endocrinol* 2017;451:80-7.
19. Damasceno LE, Prado DS, Veras FP, Fonseca MM, Toller-Kawahisa JE, Rosa MH, *et al.* PKM2 promotes Th17 cell differentiation and autoimmune inflammation by fine-tuning STAT3 activation. *J Exp Med* 2020;217:e20190613.
20. Siveen KS, Sikka S, Surana R, Dai X, Zhang J, Kumar AP, *et al.* Targeting the STAT3 signaling pathway in cancer: Role of synthetic and natural inhibitors. *Biochim Biophys Acta* 2014;1845:136-54.
21. Lee H, Jeong AJ, Ye SK. Highlighted STAT3 as a potential drug target for cancer therapy. *BMB Rep* 2019;52:415-23.
22. Ma X, Xie Y, Gong Y, Hu C, Qiu K, Yang Y, *et al.* Silibinin prevents TGFβ-induced EMT of RPE in proliferative vitreoretinopathy by inhibiting Stat3 and Smad3 phosphorylation. *Invest Ophthalmol Vis Sci* 2023;64:47.
23. Dinakar YH, Kumar H, Mudavath SL, Jain R, Ajmeer R, Jain V. Role of STAT3 in the initiation, progression, proliferation and metastasis of breast cancer and strategies to deliver JAK and STAT3 inhibitors. *Life Sci* 2022;309:120996.

**How to cite this article:** Li J, Lv Y, Xue S, Li W, Zhang X. Ailanthone inhibits bladder cancer tumor and cell proliferation, epithelial-mesenchymal transition, and activation of the Janus kinase/signal transducer and activator of transcription 3 signaling pathway. *CytoJournal*. 2025;22:16. doi: 10.25259/Cytojournal\_166\_2024

HTML of this article is available FREE at:  
[https://dx.doi.org/10.25259/Cytojournal\\_166\\_2024](https://dx.doi.org/10.25259/Cytojournal_166_2024)

**The FIRST Open Access cytopathology journal**  
 Publish in *CytoJournal* and **RETAIN** your copyright for your intellectual property  
**Become Cytopathology Foundation (CF) Member at nominal annual membership cost**  
 For details visit <https://cytojournal.com/cf-member>

**PubMed indexed**  
**FREE world wide open access**  
**Online processing** with rapid turnaround time.  
**Real time** dissemination of time-sensitive technology.  
 Publishes as many **colored high-resolution images**  
 Read it, cite it, bookmark it, use RSS feed, & many----

**CYTOJOURNAL**  
[www.cytojournal.com](http://www.cytojournal.com)  
 Peer-reviewed academic cytopathology journal